ACS APPLIED MATERIALS & INTERFACES

Research Article

www.acsami.org

Improved Adhesion of Dense Silica Coatings on Polymers by Atmospheric Plasma Pretreatment

Linying Cui,[†,‡] Alpana N. Ranade,[§] Marvi A. Matos,[§] Geraud Dubois,*[,†,⊥] and Reinhold H. Dauskardt*[,†]

[†]Department of Materials Science and Engineering and [‡]Department of Applied Physics, Stanford University, Stanford, California 94305, United States

[§]Chemical Technology Division, Boeing Research and Technology, Seal Beach, California 90740, United States

[⊥]IBM Almaden Research Center, 650 Harry Road, K-17/E-1, San Jose, California 95120, United States

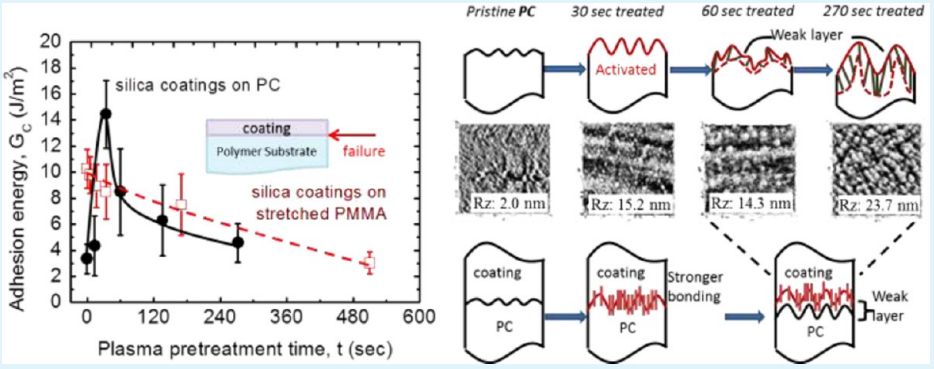

ABSTRACT: Oxygen atmospheric plasma was used to pretreat polycarbonate (PC) and stretched poly(methyl methacrylate) (PMMA) surfaces in order to enhance the adhesion of the dense silica coatings deposited by atmospheric plasma on the polymer substrates. The treatment time and chemical structure of the polymers were found to be important factors. For PC, a short treatment increased the adhesion energy, while longer treatment times decreased the adhesion. In contrast, plasma pretreatment monotonically decreased the adhesion of PMMA, and pristine PMMA exhibited much higher adhesion than the PC counterpart. We found that adhesion enhancement was achieved through improved chemical bonding, chain interdiffusion, and mechanical interlocking at the coating/substrate interface, after a short atmospheric plasma treatment. Decreased adhesion resulted from overoxidation and low-molecular-weight weak layer formation on the polymer surface by prolonged atmospheric plasma treatment. The dramatic differences in the behavior of PC and PMMA in relation to the plasma treatment time were due to their dissimilar resistance to atmospheric plasma exposure.

KEYWORDS: *adhesion, atmospheric plasma, polymer, silica coating, surface chemical state, surface morphology*

INTRODUCTION

Polymers are often coated by protective or functional coatings to extend the performance and lifetime of the final product. One of the most common coatings on polymers is silica, for the purpose of hard protective coatings,[1] permeation barriers to gas diffusion (when dense enough),[2] wettability layers (when covered by silanol groups),[3] optical layers in the fabrication of photovoltaic solar cells,[4] and corrosion-resistant layers in precision engineering (aeronautical and automotive).[1,5] However, most polymers are hydrophobic because of their major elemental chemical composition of hydrogen and carbon and have poor adhesion with hydrophilic coatings, including various oxides and nitrides.[6,7]

To improve the adhesion of hydrophilic coatings on polymers, several surface treatments of polymers have been studied. Mechanical roughening[6] and wet chemical treatment[8] are among the traditional methods. Plasma treatments by corona and low-pressure glow discharges have also been intensively studied and widely accepted in industry.[9,10] In recent years, an atmospheric-pressure plasma jet was reported for modifying polymer surfaces.[11−14] It has been shown that atmospheric plasma can increase the polymer surface energy by forming alcohol, ketone, aldehyde, carbonate, ester, and ether groups through oxidation reactions.[11,12] The surface morphology is also modified after treatment.[11,13] Because of the chemical and morphological modifications on the surface, the adhesion between the treated polymer and epoxy was reported to be significantly improved.[12,13] However, to our knowledge, there has not been any report about the important factors and different possible changes in the adhesion between an atmospheric-plasma-pretreated polymer and hydrophilic atmospheric plasma coatings.

The atmospheric plasma process has the advantage of not requiring vacuum equipment, so the initial capital investment is

Received: May 20, 2013
Accepted: August 13, 2013
Published: August 13, 2013

   dx.doi.org/10.1021/am401921k | *ACS Appl. Mater. Interfaces* 2013, 5, 8495−8504

largely decreased, and when integrated with other tools, it allows for the treatment of large and/or complex geometry substrates.[15] A better understanding of this emerging technique for improving the surface properties of polymers requires knowledge of both atmospheric plasma and adhesion mechanisms.

The principal adhesion mechanisms to polymers include (1) chemical interactions (covalent, ionic, etc.), (2) mechanical interlocking (surface topography), (3) interdiffusion of chains, and (4) other weak interatomic forces (hydrogen bonds, van der Waals forces, etc.). All of these mechanisms can be modified by atmospheric plasma treatment through the effects of cleaning, etching, chemical modification, and cross-linking of the surface.[15] Surface cleaning removes low-molecular-mass contaminants that interfere with bonding. Etching cuts the polymer chains to create more chain ends, which improve interdiffusion between the polymer and coating species at the molecular scale. At a larger length scale, etching increases the surface area and promotes mechanical interlocking. Chemical modification is also important because the newly formed polar functional groups can improve covalent-bonding and intermolecular interactions at the interface. Finally, cross-linking the surface polymer layer by ultraviolet (UV) plasma radiation can cohesively strengthen the polymer layer and potentially enhance its adhesion property.

In this study, we used oxygen atmospheric plasma to pretreat the polycarbonate (PC) and stretched poly(methyl methacrylate) (PMMA) substrates and studied their adhesion variation with hydrophilic silica coatings deposited by atmospheric plasma. We observed a factor of 4 increase in adhesion to the PC substrate with a 30 s atmospheric plasma treatment, while prolonged treatment decreased the adhesion. In contrast, plasma pretreatment monotonically decreased the adhesion of PMMA, and pristine PMMA exhibited much higher adhesion than the PC counterpart.

To explain the different behavior of the adhesion on PC and PMMA, surface studies after different amounts of atmospheric plasma exposure were performed by X-ray photoelectron spectroscopy (XPS) and atomic force microscopy (AFM). Two competing effects of atmospheric plasma treatment were observed: (1) After short atmospheric plasma exposure, the polymer surface can be modified with more polar groups and chain ends and higher surface roughness, all of which enhance a polymer's adhesion to hydrophilic coatings. (2) Plasma exposure can lead to the formation of a low-molecular-weight layer (LMWL) on the surface, especially with longer treatment. The LMWL hindered effective interaction between the coating and the bulk substrate, resulting in adhesion decrease. Interestingly, the surface modification kinetics was strongly correlated with the chemical structure of the polymer, as described in the paper.

EXPERIMENTAL METHODS

Coating Deposition. An atmospheric pressure plasma system [Surfx Technologies LLC, Redondo Beach, CA] integrated with a high-temperature precursor delivery system was employed to pretreat the plastic substrates and deposit the coating.[16] The area of the plasma showerhead was 5.1 cm^2. A total of 99.995% purity quality helium and oxygen [Praxair Inc., Santa Clara, CA] were mixed and fed into the capacitive discharge plasma. The plasma was driven by 13.56 MHz radio-frequency (RF) power. Reactive species were generated in the afterglow region of the plasma, including ground-state oxygen atoms (^3P), metastable molecular O_2 ($^1\Delta_g$ and $^1\sum_g+$), and ozone.[17] UV photons were also generated in the vicinity of the plasma source.[6,18] It was reported previously that He/O_2 atmospheric plasma can produce a variety of UV photons, such as the O I line at 130 nm and other lines from 200 to 400 nm.[6,18,19] These photons are sufficiently energetic to break organic bonds and get absorbed in a polymer surface typically a few tens of nanometers deep.[6]

A carbon-bridged precursor, 1,2-bis(triethoxysilyl)ethane [Gelest, Inc., Morrisville, PA], was used to deposit silica coatings. The precursor was vaporized at 120 °C with a vapor pressure of 1.6 Torr.[16] The precursor bubbler had helium gas flowing through at 0.1 L/min flow rate and 1 atm of pressure. The outcoming gas was a mixture of helium and saturated precursor vapor. The plasma parameters used were 30 L/min helium, 0.5 L/min oxygen, and 60 W RF power. A detailed description of the deposition conditions was given in our previous paper.[16] Coatings were deposited on silicon (100) wafers, PC [Makrolon Ltd., San Diego, CA], and military-grade stretched PMMA sheets meeting all requirements of MIL-PRF-25690. The substrate was wiped with ethanol before deposition to remove any surface contamination and dust and then dried in air for 24 h. The substrate was placed 5 mm below the plasma source and exposed to the plasma afterglow. Deposition of a uniform coating with controlled thickness was implemented through the use of an X−Y−Z stage that moved the plasma source over the substrate in a planar fashion, forming a rectangular array. The speed of the plasma source was 50 mm/s. The spacing between neighboring lines in the array was 0.3 mm.

Atmospheric Plasma Treatment of the Stretched PMMA and PC Substrates. The PC and PMMA substrates were pretreated by oxygen atmospheric plasma for different amounts of time in order to activate the surface before deposition. The same plasma conditions as those for deposition were used: 30 L/min helium, 0.5 L/min oxygen, and 60 W RF power. The substrate was placed 5 mm below the plasma source, exposed to the plasma afterglow. An X−Y−Z stage moved the plasma source over the substrate in the same fashion as that described in the deposition section above. The PC substrates were plasma-treated for 0, 15, 30, 140, and 270 s before coating deposition and for 0, 30, 60, and 270 s for surface property characterization (XPS and AFM analyses). The PMMA substrates were treated for 0, 5, 17, 34, 170, and 510 s before coating deposition and for 0, 2, 5, 10, 60, 180, and 900 s for characterization (XPS and AFM analyses).

Characterization Methods. The coating thicknesses were characterized by ellipsometry [Woollam M2000; J. A. Woollam Inc., Lincoln, NE]. Incident light (45° polarization) at the Brewster angle of the substrate was used to maximize reflection. Polarization of the reflected light versus wavelength was first taken for the coating on the silicon substrate. Software was used to fit the refractive index and absorbance of the coating by regressive analysis given the silicon substrate properties. Then a spectrum was taken for the bare polymer substrate (wavelength 250−1000 nm). Finally, a spectrum was taken for the coating on the polymer substrate. The coating thickness was fitted based on the measured refractive index and absorbance of the coating and substrate spectrum.

Chemical bonding in the coating was characterized using IR spectroscopy. The spectrum was recorded as power dispersions in KBr (reflectance mode) [Nexus 670 FT-IR; Thermo Fisher Scientific Inc., Waltham, MA]. Mid-IR (wavelength 400−4000 cm^{-1}) was probed at a resolution of 4 cm^{-1}. Coatings on silicon substrates were characterized in transmission mode at the Brewster angle of the silicon substrate.

The surface morphology of the coatings and the atmospheric-plasma-pretreated PMMA and PC were characterized by AFM [a Park Systems model XE-70 scanning probe microscope, Park Systems Inc., Santa Clara, CA]. Noncontact mode was used, with a scan area of 1.267 μm × 1.267 and 1.7 μm Z range. The root-mean-square surface roughness was obtained using the *XEI* software equipped with the AFM machine.

The chemical state of the carbon species on the polymer surface was analyzed by XPS [Physical Electronics Inc., Chanhassen, MN] within 10 min after atmospheric plasma treatment. An Al Kα (1486 eV) X-ray source was used (spot size ~1 mm, pass energy 23.5 eV, and scan range 20 eV). All of the spectra were referenced to the C 1s peak of the aliphatic C−H/C−C at 285.0 eV. The elemental composition of the coatings and the fracture surfaces after the adhesion/cohesion test was also characterized by XPS (pass energy 117.4 eV and scan range 0−1000 eV). Surface contamination was removed by argon-ion beam sputtering

before measurement of the coating composition (sputter rate 9 nm/min for typical PECVD silica coatings and sputter time 5 min).

The adhesion energy of the coating on the plastic substrate was quantified using the asymmetric double-cantilever beam (ADCB) test.[1,16,20−22] The specimens were prepared by gluing a blank thinner substrate (beam) onto a coated thicker substrate (beam). The in-plane dimensions of the specimen were 9 mm × 70 mm. Because of the availability of the thickness of the plastic sheet, the PC and PMMA specimens had different thicknesses; the PC specimen had a 4.5-mm-thick blank beam and a 5.9-mm-thick coated beam, and the PMMA specimen had a 3-mm-thick blank beam and a 6-mm-thick coated beam. The fracture tests were conducted on a micromechanical adhesion test system [DTS Delaminator Test System, DTS Co., Menlo Park, CA] in displacement control mode. The specimens were loaded (displacement rate 5 μm/s) in tension to produce controlled crack growth, followed by unloading. The load was measured simultaneously, and the adhesion energy G_c (J/m^2) was calculated from the critical value of the strain energy release rate using[1,20−22]

$$G_c = \frac{6P_c^2}{E'B^2}\left[\left(\frac{a}{h_1} + 0.64\right)^2\frac{1}{h_1} + \left(\frac{a}{h_2} + 0.64\right)^2\frac{1}{h_2}\right] \quad (1)$$

where P_c is the load when the load−displacement curve deviated from linearity until the initial crack extension, E' the plane-strain Young's modulus of the substrate, B the substrate width, a the crack length, and h_1 and h_2 the substrate thicknesses. Application of the technique to thin hard coatings on softer substrates of type similar to that in the present study has been previously reported.[1,16]

RESULTS AND DISCUSSION

Uniform dense silica coatings of ∼600 nm thickness were deposited on the PC and PMMA substrates by atmospheric plasma. The adhesion of the coatings was remarkably affected by the atmospheric plasma pretreatment time and the chemical structure of the substrate. XPS and AFM analyses correlated the surface chemical and morphological changes with the adhesion variations, revealing two competing effects of atmospheric plasma pretreatment on the polymer's adhesion.

Coating Properties. The deposition rate of the coating was 116 ± 20 nm/min on PC and 106 ± 22 nm/min on PMMA. The surface roughness of the coatings was below 1 nm on all substrates. Characterization of the coatings' atomic and chemical properties as well as the density and Young's modulus was previously reported.[16] The silica coating was composed of 5 atom % of carbon, 32 atom % of silicon, and 63 atom % of oxygen by XPS measurement. Hydrogen was not included in the atomic composition calculation because of limitations of the technique. The Si−O−Si network structure was formed in the coating, as revealed by its IR spectrum.[16] The carbon residues were in the form of Si−O−C and C═O, suggesting that the carbon bridge in the precursor molecule was oxidized under the current deposition conditions. The Si−OH stretching mode was also observed in the IR spectrum, as a common feature for as-deposited low-temperature PECVD silica coatings.[23] The coating had a density of 1.833 g/cm^3 and a Young's modulus of 22.7 ± 2.3 GPa, much higher than those of the commercial polysiloxane coatings prepared by the sol−gel process.[1] The water contact angle of the coating was 37°, confirming that the coating was hydrophilic.

Effect of Plasma Pretreatment of the PC Substrate on Adhesion to Silica Coating. The adhesion of the dense silica coating to the PC substrate was evaluated by the ADCB test. We observe a significant enhancement of adhesion by short atmospheric plasma pretreatment, while longer pretreatment reduces the adhesion gradually. The adhesion energies to the 0, 15, 30, 60, 140, and 270 s atmospheric-plasma-pretreated PC substrates are 3.5 ± 1.2, 4.4 ± 2.3, 14.5 ± 2.6, 8.5 ± 3.3, 6.3 ± 2.7, and 4.6 ± 1.5 J/m^2, respectively (Figure 1). XPS surface analysis

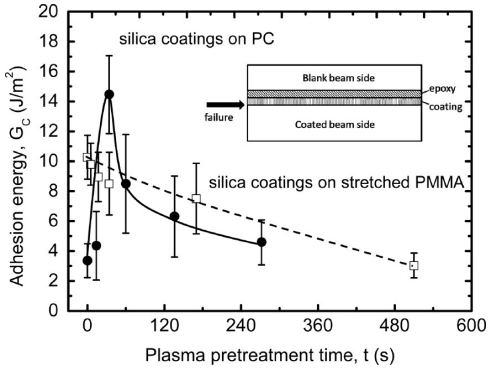

Figure 1. Adhesion energy of the dense silica coating on the PC and PMMA substrates with different amounts of atmospheric plasma pretreatment time.

showed that all of the failures are adhesive: the original blank side had silicon, oxygen, and carbon elements by XPS, while the original coated side had carbon and oxygen elements. The carbon species on the original blank side can be from the coating itself, the developing LMWL, and hydrocarbon and CO_2 absorbents from the air. In order to understand the underlying mechanism for this trend, the chemical and morphological properties of the atmospheric-plasma-treated PC substrate were characterized by XPS and AFM.

XPS Analysis of the Chemical State Evolution of the PC Surface. The chemical states of surface carbon species were analyzed to elucidate the chemical interaction between the PC surface and oxygen atmospheric plasma. The C 1s XPS spectrum of pristine PC is plotted in Figure 2a(i), which can be deconvoluted to six Gaussian/Lorentzian functions corresponding to different carbon bonding states:[24−28] (1) 284.5 eV, aromatic C−H; (2) 285.0 eV, aliphatic C−H/C−C; (3) 286.2 eV, aromatic C−O; (4) 290.4 eV, O_2C═O; (5 and 6) 291.3 and 292.5 eV, two shakeup satellites for the $\pi \rightarrow \pi^*$ transition of the carbon atoms in the aromatic ring. [Labeling of the carbon atoms is shown in the inset of Figure 2a(i).] After oxygen atmospheric plasma treatment, two additional peaks appear[24−27] [Figure 2a(ii)]: (7) 287.5 eV, aliphatic C═O and O−C−O; (8) 288.8 eV, O−C═O.

The oxidation of PC follows three steps with increasing plasma treatment time, as shown by the evolution of the percentage of the different carbon components (Table 1 and Figure 2b). Within the first 30 s of treatment, there are sharp drops of the aliphatic C−H/C−C and aromatic C−H species, together with the diminishing $\pi \rightarrow \pi^*$ shakeup satellites. This suggests that the alkyl groups and aromatic rings are rapidly oxidized or ring-opened by oxygen atmospheric plasma, forming carbonates, esters, O−C−O and carbonyl groups, and oxidized aromatic rings.[24−27]

At longer exposure from 30 to 60 s, oxidation saturates at the aliphatic C−H/C−C group sites but persists at the aromatic ring sites. More rings are oxidized (decrease of the aromatic C−H peak and $\pi \rightarrow \pi^*$ shakeup satellites) or opened (decrease of the sum of the aromatic C−H and C−O peaks). It is also worth noting that the carbonate and ester species increase faster than the carbonyl and O−C−O groups, suggesting that oxidation

dx.doi.org/10.1021/am401921k | ACS Appl. Mater. Interfaces 2013, 5, 8495−8504

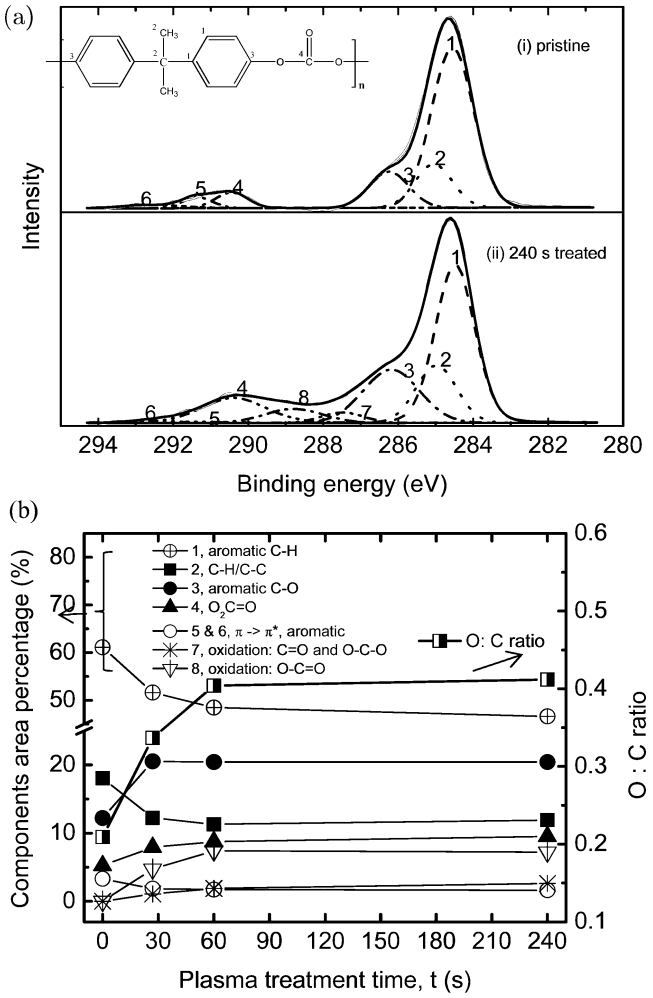

Figure 2. (a) C 1s XPS spectrum of (i) pristine PC and (ii) 240 s atmospheric-plasma-treated PC, deconvoluted to different carbon bonding states. (b) O:C ratio and the area percentage of different components in the C 1s envelope of PC in relation to oxygen atmospheric plasma treatment time.

proceeds to higher oxidation states at many sites. We believe that at this stage many PC chains are broken.

From 60 to 240 s exposure to atmospheric plasma, the percentages of all of the components stay almost the same. The overall O:C atomic ratio is also stable. This suggests that, at 60 s atmospheric plasma exposure, the top 10 nm of the PC surface (the probing depth of XPS is ~10 nm) has reached the maximum oxidation state and many polymer chains have been broken. Further oxidation of these low-molecular-weight oligomers results in the formation of highly volatile species that would easily leave the surface. In other words, after 60 s of atmospheric plasma treatment, surface etching balances chemical modification in the 10 nm surface layer (the penetration depth of the X-ray beam). However, the LMWL can grow thicker than 10 nm after longer plasma treatment, as shown by the AFM results below. The formation of a LMWL on prolong-treated PC has been reported previously.[24]

AFM Analysis of the Morphology Evolution of the PC Surface. Similar to the surface chemical state, the surface morphology of PC also exhibits changes in three stages. In order to probe the LMWL that we proposed to form after long plasma treatments, we compare the AFM images of the plasma-treated PC before and after rinsing with ethanol (Figure 3). If the LMWL

Table 1. Fitting Parameters for the C 1s Envelope of PC[a]

	peak number								
	1	2	3	4	5 and 6	7	8	O:C ratio
bond	aromatic C−H	aliphatic C−H/C−C	aromatic C−O	$O_2C{=}O$	$\pi \rightarrow \pi^*$, aromatic	oxidized: aliphatic C=O and O−C−O	oxidized: O−C=O	
peak position (eV)	284.5	285.0	286.2	290.4	291.3, 292.5	287.5	288.8	
peak area percentage (%) after atmospheric plasma treatment								
0 s	61.1	18.1	12.2	5.3	3.3	0	0	0.209
30 s	51.6	12.3	20.5	7.9	1.9	1.1	4.7	0.337
60 s	48.5	11.3	20.4	8.7	1.7	1.9	7.4	0.404
240 s	46.6	11.9	20.4	9.5	1.6	2.6	7.2	0.412

[a]The percentage of the different carbon species and the O:C ratio in relation to the atmospheric plasma treatment time.

dx.doi.org/10.1021/am401921k | ACS Appl. Mater. Interfaces 2013, 5, 8495−8504

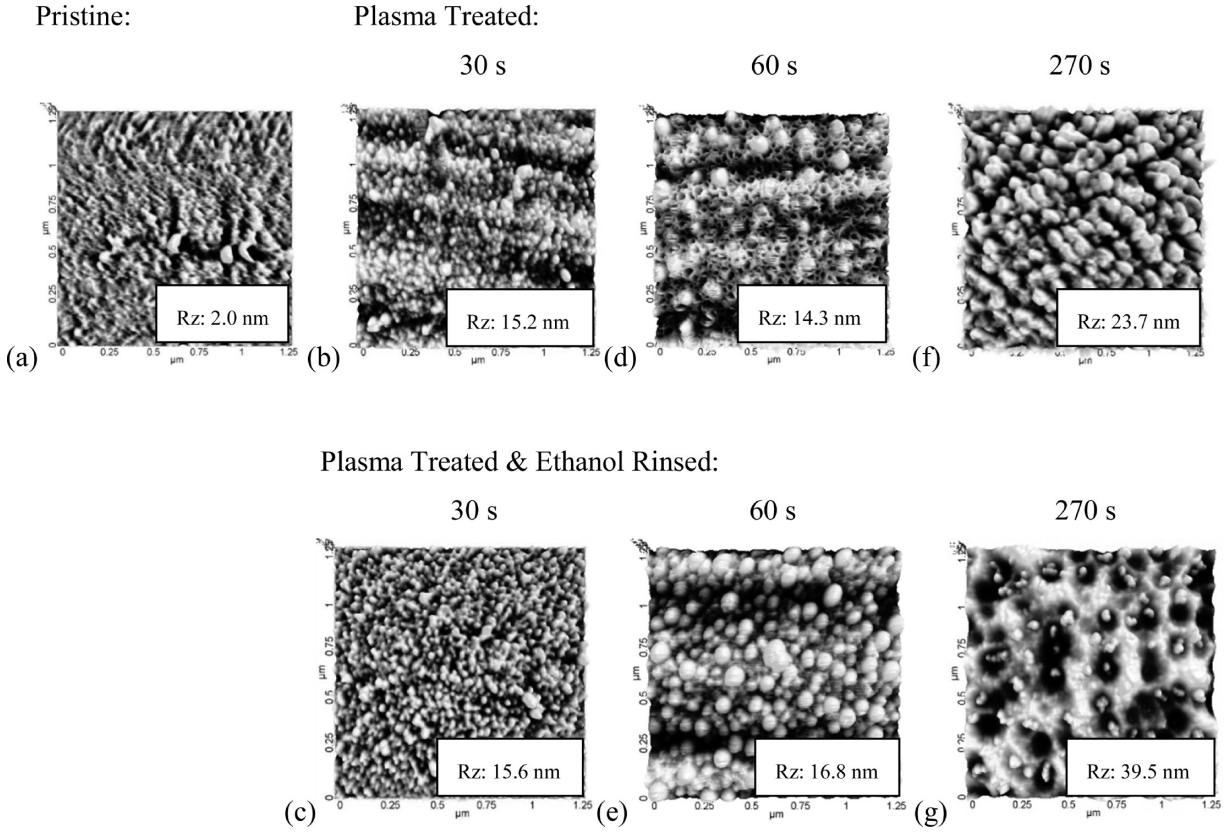

Figure 3. AFM images of PMMA: (a) pristine; after atmospheric plasma treatment of (b) 30, (d) 60, and (f) 270 s; corresponding (c) 30, (e) 60, and (g) 270 s plasma-treated and ethanol-rinsed surfaces. Rz is the arithmetic average of the five highest peaks and five lowest valleys in a selected 400 nm × 400 nm region.

is formed, the surface after rinsing should appear significantly different under AFM.

The PC sheet in this study is manufactured by injection molding from PC resins. The pristine PC surface has hill features of ∼40 nm width and ∼1 nm height (Figure 3a), probably resulting from the inhomogeneity of the melted PC gel at the nanoscale.

After 30 s of atmospheric plasma exposure, the height of the 40-nm-wide hills increases from ∼1 to ∼8 nm (Figure 3b), indicating significant surface modification. The flat background has a higher modification rate than the side walls of the hills because it is perpendicular to the plasma flow and thus receives a higher plasma afterglow dose per unit area. The surface roughness increases from 0.3 to 4.2 nm. The surface morphology is almost the same before and after ethanol rinse (Figure 3b,c), so it is likely that LMWL has not yet been formed.

When the plasma treatment is extended to 60 s, voids begin to form and larger-sized hills of ∼80 nm width and ∼7 nm height (Figure 3d) replace the 40-nm-wide hills. The LMWL has started to form, and the very top layer, which contains voids, can be rinsed off by ethanol (Figure 3e).

There are multiple possible reasons for the emergence of the larger 80-nm-wide hills. One is that the PC sheet is not homogeneously cross-linked at the nanoscale. Because the PC sheet is manufactured from the melted PC resins, the intersection region of different resins may be less cross-linked than the inner part of the resin because of the different cross-linking conditions for manufacturing the resin and sheet. The fluctuation of the density and scattering of the reaction center or catalyst during resin preparation can also lead to inhomogeneity at the nanoscale. The less cross-linked region of the polymer is likely to form low-molecular-weight oligomers and voids at first because fewer oxidation/disentanglement reactions are required. The 80-nm-wide hills are probably from the more cross-linked region. Another possibility is that UV radiation from the plasma cross-links the surface polymer chains and changes the morphology. Cross-linking polypropylene in a surface skin of ∼30 nm thickness by oxygen plasma was reported previously.[29] Note that melting is not possible at the current conditions because the plasma temperature at the current conditions is 80 °C, much lower than the glass transition temperature of PC at 148 °C.[30] Nevertheless, the 80-nm-wide hills are the main surface features beyond 60 s of atmospheric plasma treatment, as shown below.

After 270 s of plasma exposure, a thicker LMWL is formed. Interestingly, the surface features (Figure 3f) are also hills of ∼80 nm width. Compared to the 60 s plasma-treated surface (Figure 3d), the void-containing layer has been oxidized to volatile species. The height of the hills increases from ∼7 to ∼12 nm because of a larger plasma dose on the flat background than the side walls of the hills, as discussed above.

An ethanol rinse leaves narrower hills of ∼40 nm width (Figure 3g). This morphology looks like removal of a skin of ∼20 nm thickness from the side walls of the 80-nm-wide hills, leaving the 40-nm-wide cores. The hill height increases from ∼12 to ∼20 nm, suggesting that an additional 8-nm-thick layer is removed from the background compared to the hill side, so the total thickness of the LMWL on the flat background area is ∼28 nm.

The surface skin that is ethanol-soluble provides good evidence for the formation of thick LMWL by atmospheric

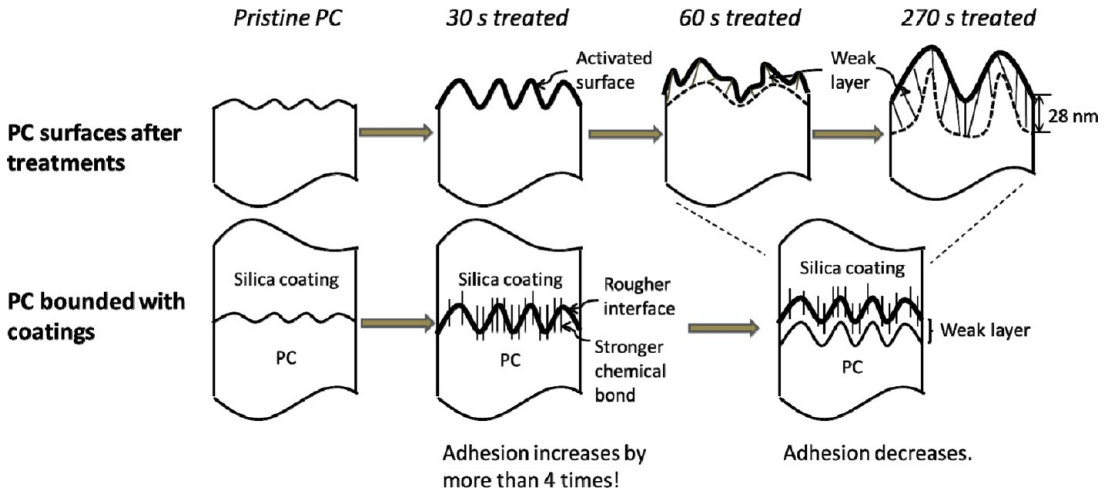

Figure 4. Schematic of PC surface modification and associated adhesion mechanisms.

plasma exposure. Forming the LMWL is a combinatorial effect of the highly reactive oxygen species and high-energy UV photons from atmospheric plasma. The high-energy UV photons are absorbed in a polymer surface typically a few tens of nanometers deep and are sufficiently energetic to break any organic bonds, which can lead to oxidation of the polymer layer,[6] especially with highly reactive oxygen species present.

Relating the Surface Chemical State and Morphology Evolutions to Adhesion Changes of PC. The XPS and AFM results shed light on the adhesion mechanisms (Figure 4), leading to the trend in Figure 1.

At a short exposure time of 30 s, oxidation of the PC substrate significantly enhances the adhesion to the silica coating. At this stage, more polar groups are formed through oxidation of the alkyl groups and aromatic rings, which improve the hydrogen-bonding and van der Waals interaction[6,7] at the interface. Additional chain ends are also created through chain scission, which increase the interdiffusion of polymer chains and coating species as another adhesion mechanism.[6,7] At the same time, the surface area increases as indicated by the 8 times increase of the height of the surface hill features, which improve the mechanical interlocking of the polymer and coating.[6,7]

More importantly, covalent bonding[6,7] is improved by the newly formed oxygen functional groups. The oxygen functional groups are more likely to form covalent bonds with the coating than the more chemically resistant aromatic groups, through reactions with plasma species, UV photons, and incoming coating precursors.[24,31,32] Last but not least, oxidation has not severely destroyed the surface polymer network, so the bulk substrate can achieve strong interaction with the coating through the modified interface.

At a longer exposure time, as the oxidation of PC proceeds, the adhesion between PC and the silica coating gradually decreases. In this regime, ring oxidation and opening become predominant, and the surface polymer network starts to degrade to form a LMWL. The LMWL of up to ~28 nm thickness significantly reduces the adhesion by hindering the interaction between the bulk PC substrate and silica coating. The formation of a LMWL by long plasma exposure was reported previously[7,24] but not correlated with quantitative adhesion changes.

The reaction kinetics of PC with oxygen atmospheric plasma gives rise to the initial increasing and then decreasing trend of adhesion with atmospheric plasma pretreatment time. Short atmospheric plasma exposure results in the nonaromatic components being mostly oxidized, forming more polar groups and chain ends. Because aromatic rings are more chemically resistant to reactive oxygen species[24,32,33] and UV radiation,[34] some of the remaining rings and partially oxidized rings help to maintain the chain network structure. This site-specific oxidation provides an exposure time window to obtain a chemically modified but not significantly weakened polymer surface to improve its adhesion to hydrophilic coatings. As oxidation proceeds to more aromatic sites, a LMWL forms and the interaction between the coating and bulk polymer substrate is weakened, resulting in a decrease in adhesion.

Effect of Plasma Pretreatment of the PMMA Substrate on Adhesion to Silica Coating. The adhesion of the dense silica coatings on PMMA was also evaluated by the ADCB test. As opposed to the adhesion behavior of PC, here the adhesion monotonically decreases with increasing plasma pretreatment (Figure 1). For the coating deposited on pristine PMMA, the fracture energy is 10.3 ± 1.5 J/m^2, comparable to the fracture energy of the commercial hard coatings on plastics.[1] The coatings deposited on 5, 17, 34, 170, and 510 s pretreated PMMA exhibit gradually decreasing fracture energies of 9.8 ± 1.4, 9.0 ± 1.7, 8.7 ± 1.2, 7.8 ± 2.4, and 3.0 ± 0.8 J/m^2, respectively. XPS analysis of the fractured surfaces shows that all failures occurred adhesively. In order to understand this monotonically decreasing trend, XPS and AFM were used to study the chemical and morphological effects of atmospheric plasma treatment on PMMA.

XPS Analysis of the Chemical State Evolution of the PMMA Surface. The bonding states of surface carbon atoms were analyzed to reveal the chemical effect of atmospheric plasma treatment on PMMA. The C 1s XPS spectrum of pristine PMMA is plotted in Figure 5a(i), which can be deconvoluted to four Gaussian/Lorentzian functions corresponding to different carbon bonding states:[35] (1) 284.9 eV, aliphatic C−C/C−H; (2) 285.7 eV, the quaternary carbon atom in the α position to the ester group; (3) 286.8 eV, the methyl group carbon single-bonded to an oxygen atom; (4) 288.9 eV, carboxylic O−C═O. [Labeling of the carbon atoms is shown in the inset of Figure 5a(i).] After oxygen atmospheric plasma treatment, two additional peaks appear[36,37] (Figure 5a(ii): (5) 287.2 eV, free carbonyl groups C═O; (6) 289.8 eV, carbonate groups O_2C═O. Maximum oxidation is reached within 10 s of treatment (Table 2 and Figure 5b), compared to 60 s for the PC surface.

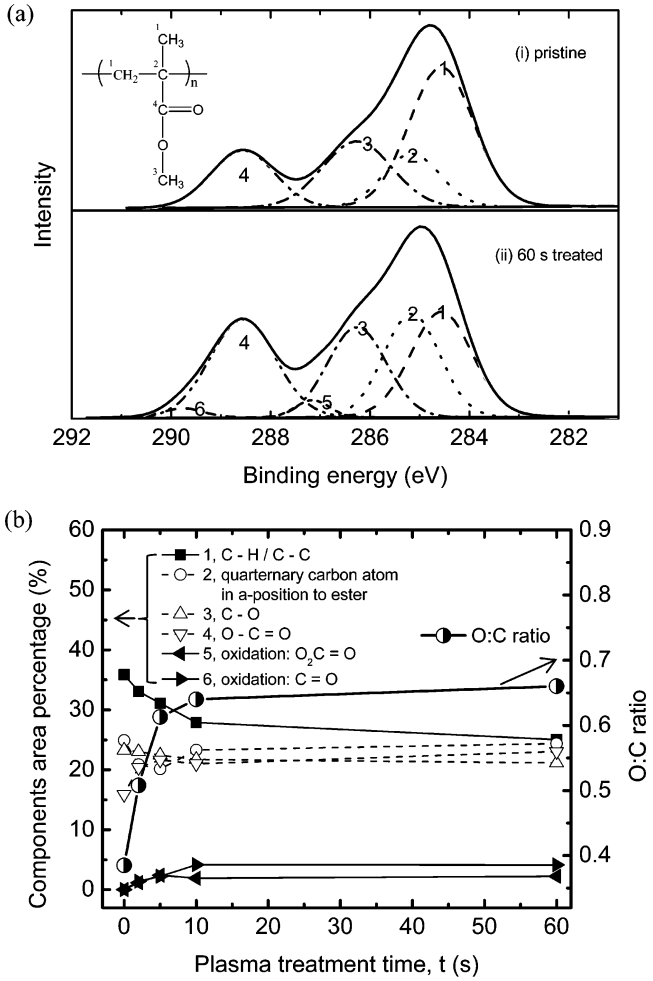

Figure 5. (a) C 1s XPS spectrum of (i) pristine PMMA and (ii) 60 s atmospheric-plasma-treated PMMA, deconvoluted to different carbon bonding states. (b) O:C ratio and area percentage of different components in the C 1s envelope of PMMA in relation to the oxygen atmospheric plasma treatment time.

The much higher sensitivity of PMMA to oxygen atmospheric plasma is due to the absence of aromatic rings in the backbone.[32]

The atmospheric plasma modification of PMMA follows only two steps (Table 2). In the first 10 s of treatment, oxidation of the side chain and nonaromatic backbone leads to a dramatic drop of the aliphatic C−H/C−C species and a significant increase of the carbon species in higher oxidation states: the ester carbon increases by 3.1%, and the free carbonyl and carbonate groups grow from 0 to 2.2% and 4.1%, respectively. The O:C ratio increases from 0.385 to 0.640.

Beyond the initial 10 s, the area percentages of the different carbon components become almost constant. The richness of carbon in high oxidation states indicates that many polymer chains have been broken to form low-molecular-weight oligomers. At this stage, surface oxidation has reached a maximum and further exposure leads to the formation of highly volatile species, resulting in a balance between surface chemical modification and etching.

AFM Analysis of the Surface Morphology Evolution and the Revealed Adhesion Mechanisms of PMMA. The different adhesion trend for PMMA compared to that for PC can be understood by its oxidation kinetics (the previous section) and morphology evolution, as revealed by AFM (Figure 6).

Pristine PMMA has better adhesion to atmospheric-plasma-deposited hydrophilic silica coatings than the plasma-pretreated PMMA and pristine PC. The high adhesion is due to plasma exposure in the initial stage of coating deposition before a uniform coating has covered the substrate. Given the coating deposition rate of ∼110 nm/min, there is direct plasma exposure for a few seconds. That amount is enough to chemically activate PMMA because 2 s of plasma treatment can already create many new surface polar groups, which significantly improve the van der Waals, hydrogen, and covalent bonding[6,7] with the hydrophilic silica coating (Figure 7).

The difference in surface morphologies of pristine (Figure 6a) and 5 s plasma-treated (Figure 6b) PMMA also confirms the high sensitivity of PMMA to atmospheric plasma exposure. The larger surface features on 5 s plasma-treated PMMA indicate that many surface polymer chains have been chemically modified or broken to even out the smaller features on the pristine surface. The newly created chain ends can improve adhesion by promoting the interdiffusion between the polymer chains and coating species (Figure 7). After ethanol rinsing and drying (with N_2 gas flow; Figure 6c), the surface morphology changes again, suggesting the flexibility of the surface polymer chains. The LMWL is not likely to form at this stage because surface oxidation has not been completed.

When atmospheric plasma treatment extends from 10 to 180 s, the adhesion only decreases slowly although oxidation of the top

Table 2. Fitting Parameters for the C 1s Envelope of PMMA[a]

	peak number						
	1	2	3	4	5	6	O:C ratio
bond	C−H/C−C	quaternary carbon atom in the α position to the ester group	C−O	O−C=O	oxidized: C=O	oxidized: O_2C=O	
peak position (eV)	284.6	285.2	286.3	288.6	287.2	289.8	
peak area percentage (%) after atmospheric plasma treatment							
0 s	39.9	20.9	20.3	19.9	0	0	0.385
2 s	33.2	20.8	23.0	20.4	1.2	1.4	0.508
5 s	31.1	20.2	22.4	21.7	2.4	2.2	0.613
10 s	27.9	23.3	21.7	21.0	1.9	4.2	0.640
60 s	25.1	24.4	21.2	23.0	2.2	4.1	0.660

[a]The percentage of the different carbon species and the O:C ratio in relation to the atmospheric plasma treatment time.

dx.doi.org/10.1021/am401921k | ACS Appl. Mater. Interfaces 2013, 5, 8495−8504

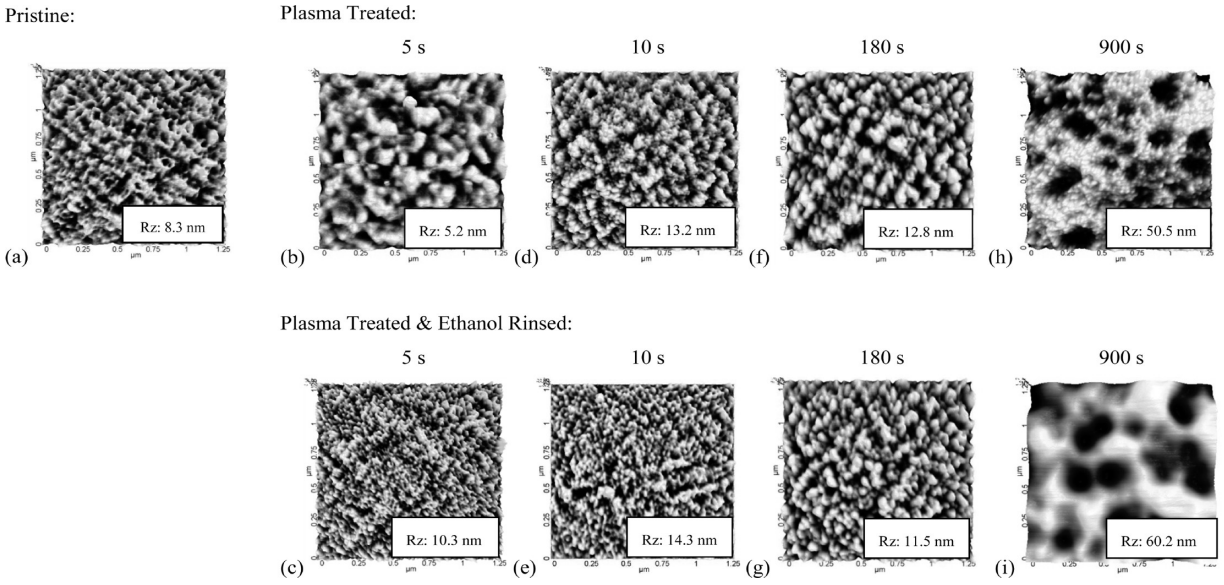

Figure 6. AFM images of PMMA: (a) pristine; after atmospheric plasma treatment of (b) 5, (d) 10, (f) 180, and (h) 900 s; corresponding (c) 5, (e) 10, (g) 180, and (i) 900 s plasma-treated and ethanol-rinsed surfaces. Rz is the arithmetic average of the five highest peaks and five lowest valleys in a selected 400 nm × 400 nm region.

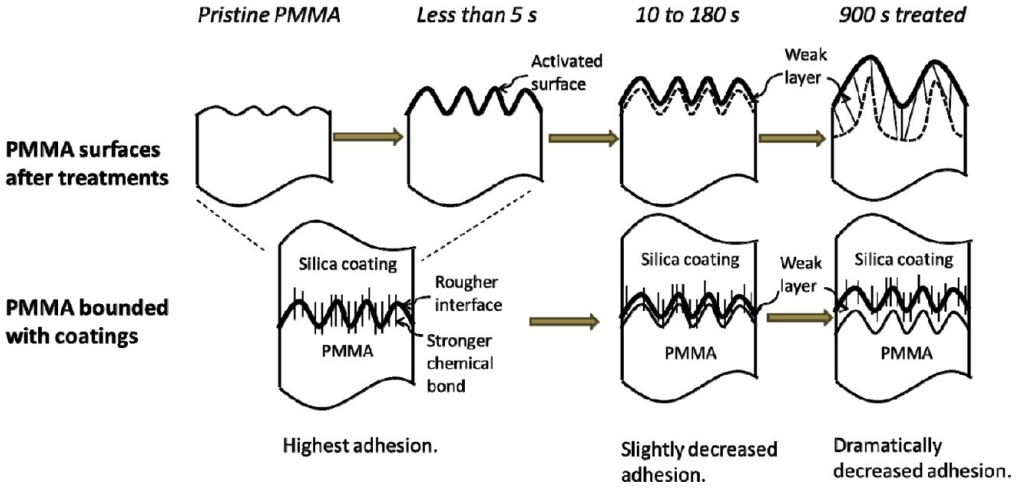

Figure 7. Schematic of PMMA surface modification and associated adhesion mechanisms.

10 nm PMMA layer has saturated (the probing depth of XPS is ~10 nm). Interestingly, the surface morphology does not change much as well, even after an ethanol rinse (Figure 6d–g), suggesting insignificant residual species accumulation to reduce adhesion. That is because complete oxidation of PMMA takes many fewer steps than that of PC, and thus the PMMA etch rate is fast enough to prevent significant accumulation of the intermediate oxidation species to form thick LMWL.

The slowly decreasing trend can be explained by the morphology change after 900 s of atmospheric plasma treatment (Figure 6h,i). Over prolonged plasma exposure, the bombardment of high-energy plasma species, such as high-energy UV photons, on the soft and damaged PMMA surface leads to pits of tens of nanometers deep (Figure 5h). A similar pit formation phenomenon was observed during plasma etching of low-*k* materials.[38] The deeper etching with pit formation leads to LMWL, which can be removed by an ethanol rinse (Figure 6i). Because pit formation is a slow process, as shown by AFM, it can be correlated to the slow decrease of adhesion for PMMA with longer plasma treatment (Figure 7).

Comparison between the PC and PMMA Substrates and with the Literature Report. Upon comparison of the reaction kinetics of PMMA and PC with oxygen atmospheric plasma, it is found that the different sensitivities of the chemical groups to reactive oxygen species give rise to different adhesion trends. For PMMA, the alkyl and ester groups that constitute the polymer side chain and backbone are both very sensitive to reactive oxygen species, so the side chain and backbone were rapidly oxidized at the same time.[13,37] Correspondingly, the surface is quickly activated, and at almost the same time, LMWL starts to accumulate. This leads to high adhesion of pristine PMMA to plasma coatings and slowly decreasing adhesion with plasma pretreatment (Figure 7). In contrast, the high resistivity of the aromatic group in the PC backbone decouples surface activation from LMWL formation. By a short plasma exposure, most of the nonaromatic components are oxidized, but the aromatic ring in the backbone helps to maintain the chain network because of its much slower oxidation process. So, a significant increase of adhesion is observed as a result of surface activation. In the LMWL formation stage that follows, oxidation

of the aromatic group takes more steps than that of the alkyl and ester groups, so more oxidation intermediates are accumulated to form thick LMWL, resulting in a sharp drop in adhesion (Figure 4).

This comparison suggests that constructing a less oxygen-sensitive backbone, such as incorporating aromatic rings in the backbone, is important for using atmospheric plasma to enhance polymers' adhesion to hydrophilic coatings. In this way, oxidation of the polymer side chain and backbone can be decoupled to different time scales, allowing for a time window to form a substrate surface rich in polar groups and chain ends with a maintained chain network.

It is also worth noting that using higher plasma powers of up to 80 W to pretreat the PC and PMMA substrates resulted in the same trends but at shorter times. However, when the plasma power was too high (≥100 W for our system), the plasma temperature increased to above the glass transition temperature of the polymer substrate.

There are some previous studies about the effect of oxygen plasma treatment of aromatic polymers and PMMA[12,13,39] on their adhesion to epoxy and resins. In one study using atmospheric oxygen plasma,[11] the adhesion of aromatic polymers to epoxy increased after plasma treatment. Chain scission[11,12,40] and LMWL formation[11,24] were observed, but no adhesion drop after longer treatment was reported. In another study,[7] which compared the treatments of low- and atmospheric-pressure plasmas, the authors reported that the low-pressure plasma treatment increased the adhesion with extended treatment time but prolonged atmospheric-pressure plasma treatment decreased the adhesion to epoxy. We believe that these different observations result from the nature of the epoxy and the thickness of the LMWL. If the epoxy can penetrate the LMWL to interact with the bulk substrate, the adhesion increases with increasing treatment time. Conversely, if the epoxy cannot penetrate LMWL to bond well with the bulk substrate, adhesion decreases. In our case, we deposited plasma coatings on polymeric substrates. It appears that the gas-phase-deposited coating is sensitive to the presence of LMWL, which significantly hinders interaction between the coating and bulk substrate and reduces adhesion.

CONCLUSION

Oxygen atmospheric plasma pretreatment was explored to improve the adhesion of PC and PMMA to plasma-deposited hydrophilic silica coatings. The treatment time and polymer chemical structure are found to be important factors. For PC, a short treatment of 30 s increased the adhesion energy by a factor of 4, while longer treatment decreased the adhesion gradually. In contrast, a monotonically decreasing trend of adhesion with longer plasma treatment was observed for PMMA, with the starting adhesion energy much higher than that in the PC case.

The chemical state and morphology of the atmospheric-plasma-treated surfaces were characterized to understand these trends. At short exposure times, the formation of surface polar groups, additional chain ends, and increased surface roughness are found to improve adhesion through covalent-bonding, hydrogen-bonding, and van der Waals interactions, chain/coating species interdiffusion, and mechanical interlocking for both PC and PMMA.

If the polymer is highly sensitive to oxidation, which is the case for PMMA, plasma exposure during the initial stage of plasma coating deposition can be sufficient to enhance adhesion. If the polymer is more resistant to reactive oxygen species, for instance, because of the presence of aromatic rings in the PC backbone, a moderate atmospheric plasma pretreatment can decouple surface activation from LMWL formation and significantly enhance adhesion. Nevertheless, if the treatment time is too long, overoxidation of both the PC and PMMA surfaces can happen, which leads to LMWL formation and reduced adhesion. These results point out the importance of the plasma pretreatment time and polymer chemical structure for adhesion enhancement.

AUTHOR INFORMATION

Corresponding Authors

*E-mail: gdubois@us.ibm.com. Phone: 408-927-1584.

*E-mail: dauskardt@stanford.edu. Phone: 650-725-0679. Fax: 650-725-4034.

Notes

The authors declare no competing financial interest.

ACKNOWLEDGMENTS

The work was supported, in part, by the Director, Office of Energy Research, Office of Basic Energy Sciences, Materials Sciences Division of the U.S. Department of Energy, under Contract DE-FG02-07ER46391, and by the Boeing Co.

REFERENCES

(1) Kamer, A.; Larson-Smith, K.; Pingree, L. S. C.; Dauskardt, R. H. *Thin Solid Films* **2011**, *519*, 1907−1913.

(2) Erlat, A. G.; Spontak, R. J.; Clarke, R. P.; Robinson, T. C.; Haaland, P. D.; Tropsha, Y.; Harvey, N. G.; Vogler, E. A. *J. Phys. Chem. B* **1999**, *103*, 6047−6055.

(3) Zhu, P. X.; Teranishi, M.; Xiang, J. H.; Masuda, Y.; Seo, W. S.; Koumoto, K. *Thin Solid Films* **2005**, *473*, 351−356.

(4) Brown, M. D.; Suteewong, T.; Kumar, R. S. S.; D'Innocenzo, V.; Petrozza, A.; Lee, M. M.; Wiesner, U.; Snaith, H. J. *Nano Lett.* **2010**, *11*, 438−445.

(5) Lionti, K.; Toury, B.; Boissière, C.; Benayoun, S.; Miele, P. *J. Sol−Gel Sci. Technol.* **2013**, *65*, 52−60.

(6) Liston, E. M.; Martinu, L.; Wertheimer, M. R. *J. Adhes. Sci. Technol.* **1993**, *7*, 1091−1127.

(7) Shenton, M. J.; Lovell-Hoare, M. C.; Stevens, G. C. *J. Phys. D: Appl. Phys.* **2001**, *34*, 2754−2760.

(8) Kruse, A.; Kruger, G.; Baalmann, A.; Hennemann, O. D. *J. Adhes. Sci. Technol.* **1995**, *9*, 1611−1621.

(9) Goldman, M.; Goldman, A.; Sigmond, R. S. *Pure Appl. Chem.* **1985**, *57*, 1353−1362.

(10) Klemberg-Sapieha, J. E.; Martinu, L.; Sapieha, S.; Wertheimer, M. R. In *The Interfacial Interactions in Polymeric Composites*; NATO-ASI, Series E: Applied Sciences; Akovali, G., Ed.; Kluwer: Dordrecht, The Netherlands, 1993; Vol. *230*, pp 201−222.

(11) Gonzalez, E.; Hicks, R. F. *Langmuir* **2009**, *26*, 3710−3719.

(12) Gonzalez, E.; Barankin, M. D.; Guschl, P. C.; Hicks, R. F. *Langmuir* **2008**, *24*, 12636−12643.

(13) Gonzalez, E.; Barankin, M. D.; Guschl, P. C.; Hicks, R. F. *Plasma Processes Polym.* **2010**, *7*, 482−493.

(14) Gonzalez, E.; Barankin, M. D.; Guschl, P. C.; Hicks, R. F. *IEEE Trans. Plasma Sci.* **2009**, *37*, 823−831.

(15) Pappas, D. *J. Vac. Sci. Technol., A* **2011**, *29*, 020801.

(16) Cui, L.; Ranade, A. N.; Matos, M. A.; Pingree, L. S.; Frot, T. J.; Dubois, G.; Dauskardt, R. H. *ACS Appl. Mater. Interfaces* **2012**, *4*, 6587−6598.

(17) Jeong, J. Y.; Park, J.; Henins, I.; Babayan, S. E.; Tu, V. J.; Selwyn, G. S.; Ding, G.; Hicks, R. F. *J. Phys. Chem. A* **2000**, *104*, 8027−8032.

(18) Foest, R.; Kindel, E.; Lange, H.; Ohl, A.; Stieber, M.; Weltmann, K. D. *Contrib. Plasma Phys.* **2007**, *47*, 119−128.

(19) Li, G.; Li, H.-P.; Wang, L.-Y.; Wang, S.; Zhao, H.-X.; Sun, W.-T.; Xing, X.-H.; Bao, C.-Y. *Appl. Phys. Lett.* **2008**, *92*, 221504.

(20) Kanninen, M. F. *Int. J. Fract.* **1973**, *9*, 83−92.

(21) Suo, Z. G.; Hutchinson, J. W. *Mater. Sci. Eng., A* **1989**, *107*, 135−143.
(22) Anderson, T. L. *Fracture Mechanics: Fundamentals and Applications*; CRC Press: Boca Raton, FL, 2005.
(23) Nowling, G. R.; Yajima, M.; Babayan, S. E.; Moravej, M.; Yang, X.; Hoffman, W.; Hicks, R. F. *Plasma Sources Sci. Technol.* **2005**, *14*, 477−484.
(24) Muir, B. W.; McArthur, S. L.; Thissen, H.; Simon, G. P.; Griesser, H. J.; Castner, D. G. *Surf. Interface Anal.* **2006**, *38*, 1186−1197.
(25) Andrady, A. L.; Searle, N. D.; Crewdson, L. F. E. *Polym. Degrad. Stab.* **1992**, *35*, 235−247.
(26) Andrady, A. L.; Fueki, K.; Torikai, A. *J. Appl. Polym. Sci.* **1991**, *42*, 2105−2107.
(27) Clark, D. T.; Dilks, A. *J. Polym. Sci., Polym. Chem. Ed.* **1977**, *15*, 2321−2345.
(28) Lannon, J. M.; Meng, Q. *Surf. Sci. Spectra* **1999**, *6*, 75−78.
(29) Schonhorn, H.; Ryan, F. W.; Hansen, R. H. *J. Adhes.* **1970**, *2*, 93−99.
(30) Markolon polycarbonate data sheet, Bayer Material Science, 2013.
(31) Vollhardt, K. P. C.; Schore, N. E. *Organic Chemistry: Structure and Function*, 6th ed.; W. H. Freeman: Cranbury, NJ, 2011.
(32) Groning, P.; Collaud, M.; Dietler, G.; Schlapbach, L. *J. Appl. Phys.* **1994**, *76*, 887−892.
(33) Koprinarov, I.; Lippitz, A.; Friedrich, J. F.; Unger, W. E. S.; Woll, C. *Polymer* **1998**, *39*, 3001−3009.
(34) Chapiro, A. *Radiation chemistry of polymeric systems*; Interscience: New York, 1962; p 446.
(35) Girardeaux, C.; Pireaux, J.-J. *Surf. Sci. Spectra* **1996**, *4*, 134−137.
(36) Ben Amor, S.; Baud, G.; Jacquet, M.; Nanse, G.; Fioux, P.; Nardin, M. *Appl. Surf. Sci.* **2000**, *153*, 172−183.
(37) Chai, J. N.; Lu, F. Z.; Li, B. M.; Kwok, D. Y. *Langmuir* **2004**, *20*, 10919−10927.
(38) Darnon, M.; Casiez, N.; Chevolleau, T.; Dubois, G.; Volksen, W.; Frot, T. J.; Hurand, R.; David, T. L.; Posseme, N.; Rochat, N.; Licitra, C. *J. Vac. Sci. Technol., B: Microelectron. Nanometer Struct.—Process., Meas., Phenom.* **2013**, *31*, 011207.
(39) Gonzalez, E.; Barankin, M. D.; Guschl, P. C.; Hicks, R. F. *IEEE Trans. Plasma Sci.* **2009**, *37*, 823−831.
(40) Hofrichter, A.; Bulkin, P.; Drevillon, B. *J. Vac. Sci. Technol., A* **2002**, *20*, 245−250.